HPGe Validation Measurements of the Geant4 Radioactive Decay Simulations

S. Hauf[1,2], M. Kuster[2], M. Batič[3], Z.W. Bell[4], D.H.H. Hoffmann[1], G. Hoff[5], P.M. Lang[1], M.G. Pia[3], A. Weckmann[1], G. Weidenspointner[6,7], A. Zoglauer[8]

[1] Institut für Kernphysik, TU Darmstadt, Darmstadt, Germany
[2] European XFEL GmbH, Hamburg, Germany
[3] INFN Sezione di Genova, Genova, Italy
[4] Oak Ridge National Laboratory, Oak Ridge, TN, USA
[5] PUCRS, Rio Grande do Sul, Brazil
[6] Max–Planck Institute for extraterrestrial Physics – MPE, Garching, Germany
[7] Max–Planck Halbleiterlabor, Munich, Germany
[8] University of California at Berkeley, Berkeley, CA, USA

Abstract

It has become increasingly common to use Monte-Carlo simulations in the design phase of new experiments. Frequently, radioactive decays play an important role in designing and understanding e.g. space and ground based low background detectors, medical applications, material science studies and homeland security. Often hardware is not yet available and accordingly a simulation cannot always be cross-calibrated with measurements. In consequence knowledge about the accuracy of a simulation, unaltered by experimental input, can be of critical importance. Using measurements obtained from a High Purity Germanium Detector (HPGe) we have validated Geant4 for such a self-consistent application scenario, i.e. no calibration of the simulation was performed. Two different radioactive decay codes are compared: the current Geant4 implementation (G4.9.4-p04) and a new code developed within the nano5 team which offers a novel statistical sampling approach. Our results show that Geant4 simulations qualify as a predictive tool for estimating the effects of radioactive sources in the aforementioned diverse field of applications.

1 Experimental Setup

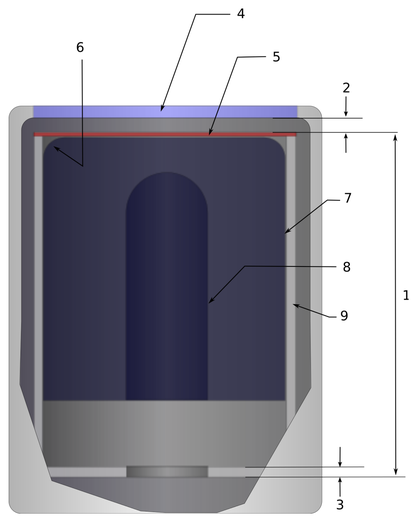

FIGURE 1: Left panel: the experimental setup consisting of a HPGe detector which is placed inside hollow lead shielding blocks shown in the center left part of the image. These blocks are the outer part of a collimator which additionally consists of a tin and a copper tube, placed around the cylindrical detector head. Additional steel shielding can be seen on the tables. The source was suspended in front of the detector by a thin wire. Not visible is the detectors's dewar. Right panel: A sketch of the HPGE-Detector's head and the inner-lying HPGe/crystal: **1** Mount cup length, **2** Distance end cap - crystal, **3** Mount cup base, **4** Beryllium entrance window, **5** Mylar insulator, **6** crystal end radius, **7** outer dead layer, **8** inner dead layer and bore, **9** Mount cup thickness. Measurements were obtained from private communication.

2 Measurements

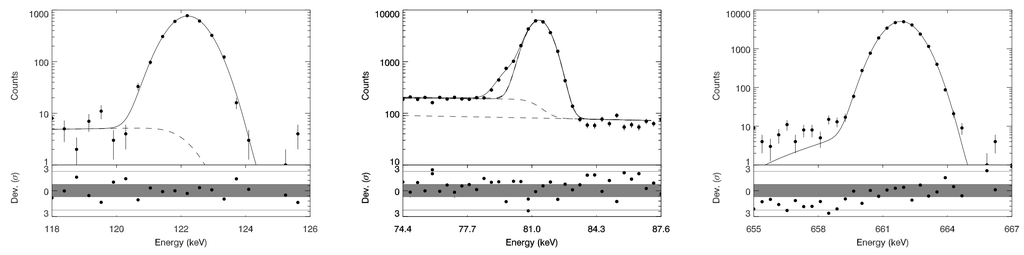

FIGURE 2: The upper panel shows measured photo peaks (dots) of ^{57}Co, ^{133}Ba and ^{137}Cs. The first plot shows how the background model includes a Compton-edge, modelled as a step-function. The second plot illustrates the ability of the fitting program, HYPERMET, to model (lines) multiple peaks in one spectrum which includes a linear part (lower dashed line) as well as Compton-component (upper dashed line). Peaks are present at $79.61\,\mathrm{keV}$ and $80.99\,\mathrm{keV}$. The third plot shows a peak which experiences a distinct exponential tail towards lower energies, resulting from incomplete charge collection. The lower panel shows the residuals in terms of σ uncertainties (solid area: 1σ, lines: 3σ) for each peak plot.

2.1 Modeling the Detector Response

Due to statistical effects and electronic noise a sharp energy signal is broadened into a Gaussian distribution

$$A\exp\left(-\frac{x-x_C}{\sigma}\right)^2 \qquad (1)$$

with amplitude A, channel x, center x_C and width σ.
Incomplete charge collection moves events from the photo peak towards lower energies, resulting in an exponential component, $exp((x-x_C)/\beta)$, with slope β. Folded with Gaussian noise of width γ this yields

$$\alpha\exp\left(\frac{x-x_C}{\beta}\right)\times\frac{1}{2}\,\mathrm{erfc}\left(\frac{x-x_C}{\gamma}+\frac{\gamma}{2\beta}\right) \qquad (2)$$

where α is a normalization factor to the amplitude A and x_C is the position of the peak's center; $erfc(u)$ is the complementary error function.
Within the detector γ-rays can scatter and exit the sensitive volume. These events result in a Compton-edge in the background. Such a step of amplitude S folded with Gaussian noise of width δ can be modeled using

$$S\times\frac{1}{2}\,\mathrm{erfc}\left(\frac{x-x_C}{\delta}\right). \qquad (3)$$

Finally, the near linear background present around the peaks can be modelled using a polynomial function:

$$B(x)=a+b\,(x-x_C)+c\,(x-x_C)^2. \qquad (4)$$

The total background is given by the sum of components 3 and 4. Background from higher energy peaks may contribute to that of lower energy ones.

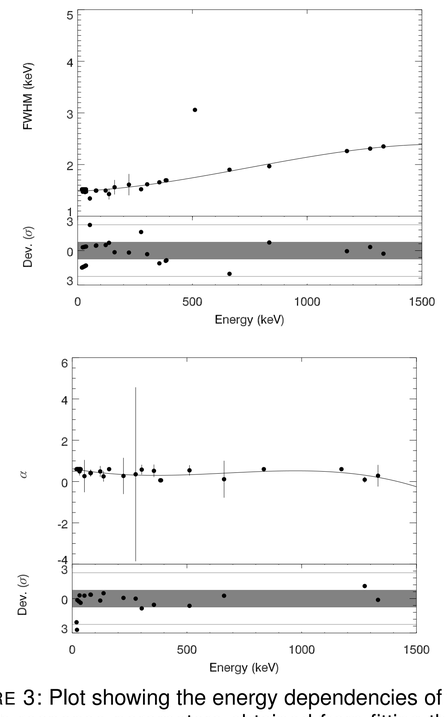

FIGURE 3: Plot showing the energy dependencies of the detector's response parameters obtained from fitting the measured photo peaks using the HYPERMET program. The lines are polynomial fits, which are needed to determine a parameter at arbitrary energies. Top: peak full-width half maximum. Bottom: parameter α. The other response parameters were determined in a similar fashion.

3 Simulations

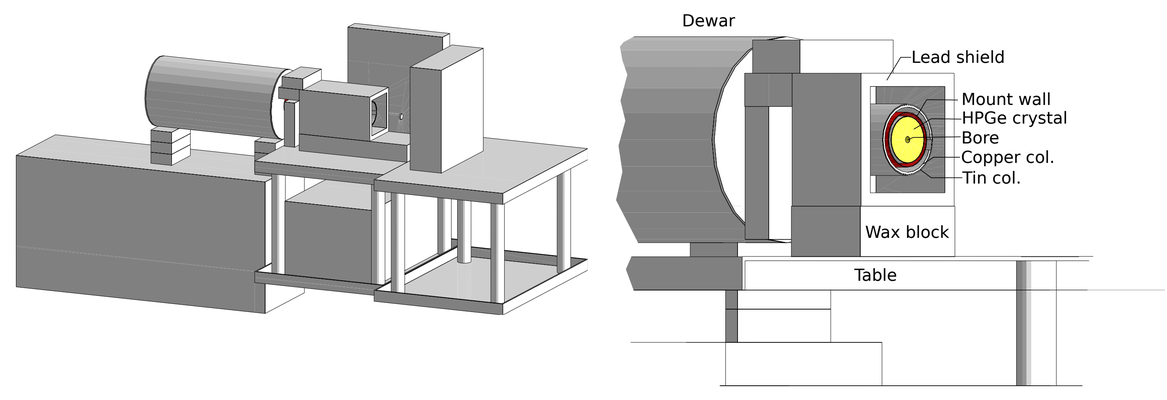

FIGURE 4: The geometrical model of the experiment used for the Geant4 simulations. The detector is located inside the hollow lead blocks at the image center, its dewar extends to the left and sits on top of borated wax blocks, which in turn are placed upon a wooden crate. The shielding is placed on top of two steel tables. Each simulation consisted of 5 Million decays of the studied isotope. The output of the simulations (event lists) was binned into spectra and processed to include the detector's response characteristics using the parameters obtained from the measurements. Two radioactive decay codes were used for the comparison: the current code of Geant4.9.4-p04 which uses a per-decay sampling approach and a novel approach which can also use statistical sampling.

4 Results - Photo Peaks

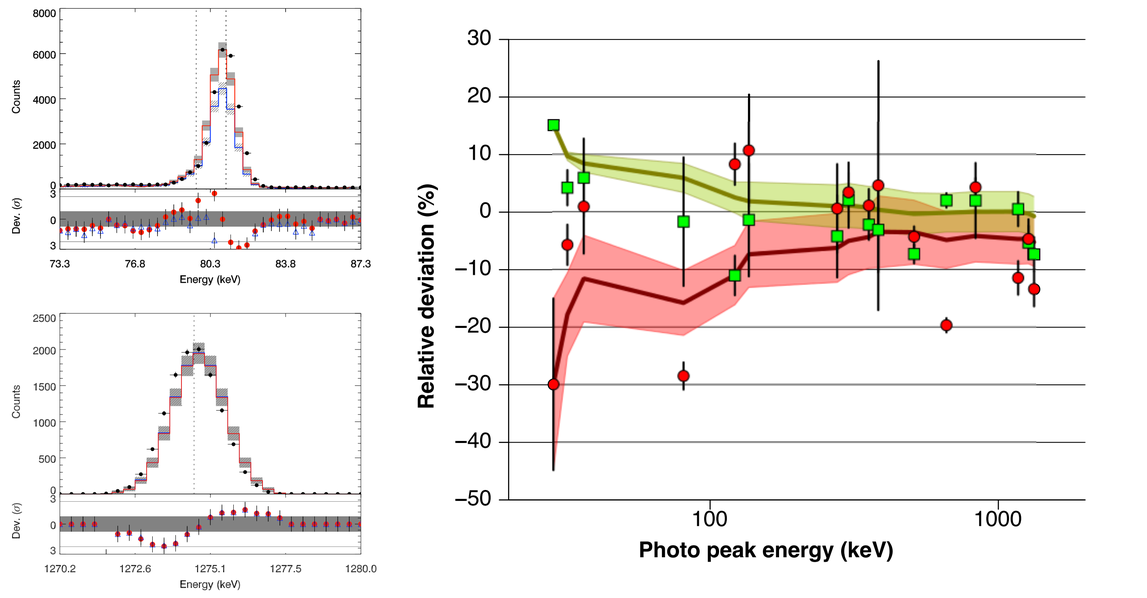

FIGURE 5: Left panel: Exemplary plots of a ^{133}Ba (top) and ^{22}Na (bottom) photo peak. The novel statistical sampling approach (red) and the current Geant4 per-decays sampling (blue) are compared to the measurement (black dots). The literature value of the peak energy is indicated as a dashed line; residuals are shown in the bottom panels. Right panel: Summary of peak intensity deviations for the novel statistical sampling approach (green) and the current per-decay sampling (red). Lines indicate the running mean deviation with shaded uncertainty areas.

5 Results - Continuum

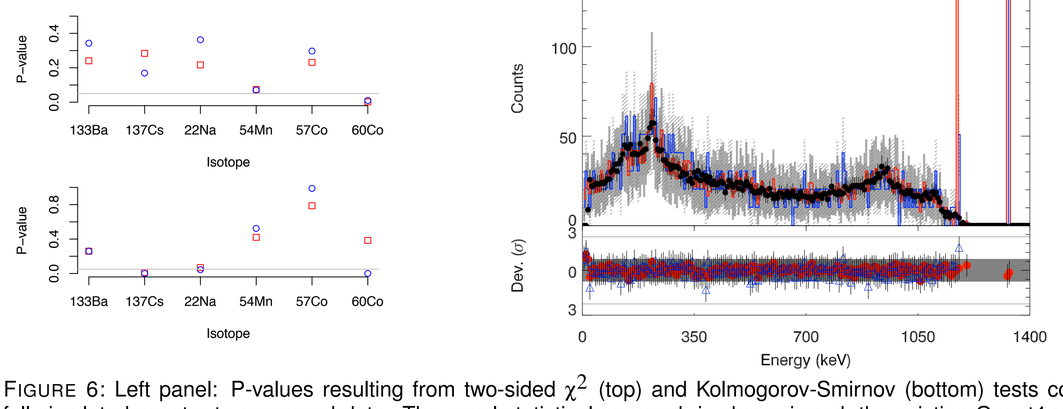

FIGURE 6: Left panel: P-values resulting from two-sided χ^2 (top) and Kolmogorov-Smirnov (bottom) tests comparing full simulated spectra to measured data. The novel statistical approach is shown in red, the existing Geant4 per-decay approach in blue. Note that except for ^{60}Co both implementations represent the data well within 95% confidence levels. Right panel: Exemplary plot of the measured ^{60}Co–spectrum (black dots) compared against simulated data using the novel (red) and current Geant4 (blue) decay code implementations. Both codes are capable of reproducing the spectra within the experimental error bounds as is apparent from the residuals in the lower panel.

6 Conclusions

Both radioactive decay implementations, the current Geant4 per-decay approach and the novel statistical approach, are capable of modeling a self-consistent HPGe-measurement of calibration sources within the experimental uncertainties. In the X-ray regime the novel implementation is slightly more accurate. Additionally, it offers computational performance benefits and is based on a modern, extensible design philosophy (**See details in talks: N28-6 and N28-7, Wednesday @ 18:00, Magic Kingdom Ballroom 4**)

Contact e-mail: steffen.hauf@xfel.eu

This work was supported by Deutsches Zentrum für Luft- und Raumfahrt under grants 50 QR 0902 and 50 QR 1102.